Self-Assembled Polystyrene Nanospheres for Plasmonic Enhancement in Biosensor Applications

K. Smith[*], C. Norville[*], M. Windham[**] and J. M. Dawson[*]
[*]West Virginia University, Morgantown, WV, USA, ksmith47@mix.wvu.edu, cnorvill@mix.wvu.edu, Jeremy.Dawson@mail.wvu.edu
[**]Louisiana State University, Baton Rouge, LA, USA, mwindh2@lsu.edu

ABSTRACT

The field of portable, point-of care biosensing has expanded in recent years to encompass a wide range of application areas. Application-specific needs of further reduced limit of detection, per-unit cost, and operational complexity continue to drive research and development efforts in the biosensor market. Label-based visible spectrum bio-sensing systems allow for an instant intensity/wavelength based visual feedback method that is common with methods of spectroscopy and electrophoresis. The drawback of these labeled visible spectrum based bio-sensors is the limit of detection is ultimately determined by the noise floor of the optoelectronic detector component. This limitation can be overcome through the addition of periodic plasmonic nano-structures (PPNS) to the surface of the sensor system being monitored by the detector. In this work, the design and fabrication of a PPNS device using self-assembled polystyrene nanospheres (NS) to achieve a ~4-fold enhancement at 565nm visible wavelength is shown.

Keywords: plasmonics, nano-spheres, nano-fabrication, bio-sensing

1 INTRODUCTION

In recent years, the role of biosensors has become increasingly versatile. In 2015, the biosensor market size was $14.8 billion, and by 2024 it is estimated to exceed $29 billion due to an increasing demand for sensing systems in home diagnostics, biodefense, biodetection, environmental monitoring, forensics, food industries, biometrics, etc. [1]. In these sensors, the detection of targets can be accomplished by a variety of sensor modalities, i.e. resonance, optical, thermal, ion-sensitive, electrochemical, etc., depending on the target metrics [2] [3] [4]. Label-free and labeled detection are two commonly used detection methods, which differ in operational characteristics. Label-free methods identify targeted molecules in the analyte material's natural state, with no external modifications to the biological material. Conversely, labeled systems instead require a label of the target material for detection, altering the natural state of the target which can affect its behavior. Intuitively, any techniques that would require the target biological to remain completely in its unaltered, natural state would be impractical for a label based method. However, label-based systems still provide distinct advantages in their ease of use, high sensitivity, and price point, leading to their implementation in many well-known applications (e.g. DNA electrophoresis) [5] [6] [7].

As previously mentioned, there are a multitude of sensing modalities. Optical methods have several characteristics which can be measured as sensor output, including optical power, fluorescence, polarization, amplitude, decay time, phase, etc. [3] [7] [8]. These senor outputs can be measured across a wide spectral range, spanning visible, ultra-violet, and infrared wavelengths. Out of these, fluorescence-based optical detection is commonly used today in many fields due to its high selectivity and sensitivity.

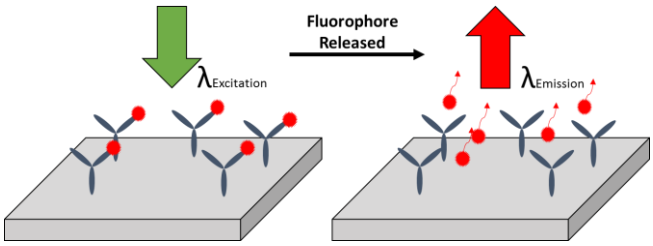

Figure 1. Process of labeled fluorescence detection, where the target analyte (blue) has been labeled with a fluorophore (red). Excited by a green laser, the fluorophore is released at a longer wavelength, red.

Label-based optical fluorescence spectroscopy uses a labeled analyte material, which is designed to bind specifically to the target molecule. An external laser source is used to excite the label attached to the target. After the label in the analyte material becomes excited, a relaxation period occurs, causing a release in energy in the form of photons at a longer wavelength. A diagram of this processes is shown above in Figure 1. While label-based optical detection methods have their own advantages and disadvantages, they are inherently constrained by the limit of detection (LOD) of the signal-detection method. The LOD is commonly defined as the concentration value of analyte material that gives a response signal of three times the standard deviation of the background signal [9]. Increasing the signal response from an analyte material, in this case photons from fluorescence, of the same concentration would assist in further decreasing the LOD of the system, thus increasing its sensitivity. This reduction additionally allows a smaller amount of analyte material to be used to achieve an equivalent signal response, as well as a reduction in analysis time for comparative results. The goal of this work is to establish a fabrication process that is cost-effective and easily implemented, while still providing a reduction in the LOD. Several methods have been employed to lower the LOD through enhancement of the fluorescent signal i.e. block surface waves, 2-D photonic crystals, flat metallic films, metallic particles, etc. [10] [11] [12] Recently the use

of plasmonics-based devices has shown the capability of increasing the fluorescent signal by up to 1000x [11] [13] [14]. This enhancement and its effect on the relationship between fluorescence response and analyte concentration is shown below in Figure 2.

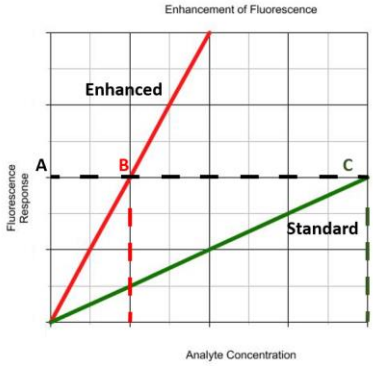

Figure 2. Graphical calibration plot showing the comparison output enhancement in a standard fluorescence spectroscopy curve. Green line is the unenhanced output curve. Red line shows higher slope due to enhancement.

These devices employ a wide variety of geometric structures, along with a multitude of methods used to fabricate those structures [11] [15] [16]. Fabrication of nanoscale features requires the use of high-accuracy patterning techniques. Polystyrene nanospheres (PNS) can be easily deposited by various methods like drop coating, spin coating, thermal Peltier evaporation, etc. to achieve sub-micron patterns and features. Additionally, these coatings do not require typical restrictions of a high-accuracy system such as e-beam lithography, including: need for high-vacuum deposition equipment, substrate size limitations, low throughput, etc. PNS deposition can be scaled per the substrate size required, and feature dimensions can be scaled per the etch rate characteristics and initial nanosphere diameter. This fabrication technique provides a cost-effective method to achieve a reduction in the LOD of biosensor devices. While this process might not achieve the highest reduction in LOD, its development is still pertinent. The simple fabrication process and price point would help lower sensitivity systems achieve similar results to their high accuracy counterparts, increasing the capability of low cost systems. This work will highlight the use of finite difference time domain (FDTD) modeling software for optimization of plasmonic lattice parameters, the fabrication of lattice structures using polystyrene nanospheres, and the characterization of their enhancement metrics.

2 DEVICE DESIGN AND SIMULATIONS

For this effort, Lumerical Solutions, Inc. FDTD software was used for the design and simulation of triangular lattice-patterned gold nanospheres to achieve optimal electric field enhancement above the periodic array. The diameter of the spheres was varied in increments of 5 nm ranging from 100 nm to 200 nm, and separate simulation runs were conducted for each sphere diameter. The boundary conditions in the *x* and *y*-directions were defined to be periodic because both the electromagnetic fields and physical structures were the same throughout the entire array. Additionally, the gold layer thickness was also varied 5 nm increments, depending on the available space. For example, a 150-nm diameter sphere would have a 25-nm maximum gold layer thickness due to the 200-nm lattice constant. This is shown in Figure 3.

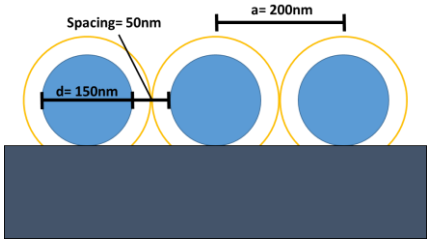

Figure 3. Spacing available for gold layer deposition on 150 nm spheres at a lattice constant of 200 nm.

An optical dipole was used as an energy source, and as configured to emit at a single wavelength of 565 nm chosen to correspond to the emission wavelength of the fluorophore being used in enhancement experiments. The lattice constant was kept constant at 200 nm. Comparison of each resulting electric field showed that optimal electric field enhancement was observed with a sphere diameter of ~125 nm, and a gold layer thickness of 25 nm. Simulation results are shown in Figure 4.

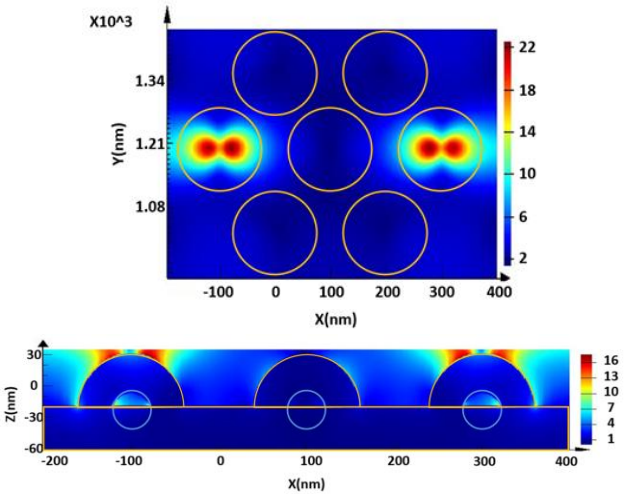

Figure 4. FDTD simulations. (Top) Top view of simulation with two dipoles directly above sphere structures and overlay outlines. (Bottom) Side view of simulated structures with two dipoles directly over sphere structures and overlay outlines.

3 FABRICATION AND TESTING

3.1 Substrate Preparation

100mm p-type silicon wafers oriented at (100) were used as a substrate for nanosphere deposition. These wafers were diced into smaller ~1cm x 1cm sections. After dicing, the samples were prepped in a sonication degreasing bath (acetone, then methanol for 5 minutes each). After sonication, the samples were thoroughly rinsed with deionized (DI) water to remove any remaining impurity and chemical residues. Samples were then dried using

pressurized nitrogen followed by 20 minutes in a dehydration baking oven at 120^{O} C to ensure all moisture was removed. Samples were then covered and allowed to cool at room temperature. In order to remove any remaining organic material, the samples were then placed in a 'Piranha' bath solution (H_2SO_4:H_2O_2,(30%), 3:1) for 30 minutes, and rinsed heavily with DI water after removal. Lastly, to promote a hydrophilic surface, the samples were placed in a 'RCA-1' clean solution (H_2O:NH_4OH(27%):H_2O_2(30%), 5:1:1) for 15 minutes, and again rinsed heavily with DI water after removal. The samples were again dried using pressurized nitrogen followed by dehydration bake. The samples were removed, covered and allowed to cool to room temperature before the nanosphere deposition.

3.2 Nanosphere Deposition

For this work, 200 nm diameter nanospheres suspended in aqueous solution from Polysciences, Inc. were used. A monolayer deposition method was developed using a thermal Peltier evaporation technique, illustrated in Figure 5.

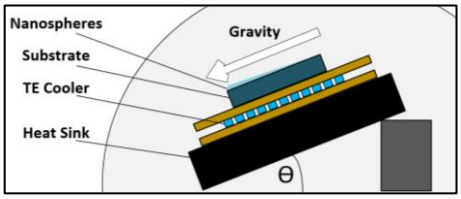

Figure 5. System set up for deposition of nanospheres using thermal Peltier evaporation.

The evaporation system was set at a temperature of 21.5^{O} C and at an angle of 10^{O}. To reduce agglomeration, a small amount of 10% concentrate sodium dodecyl sulfate (SDS) was used in the nanosphere mixture at a ratio of 99:1 (Nanosphere solution: SDS). Approximately 10 μL of polystyrene sphere solution was then deposited at the top of the substrate using a micro-pipette. The solution-covered sample was then allowed to dry on the thermal plate for 20 minutes. SEM images showing the nanosphere deposition are shown in Figure 6.

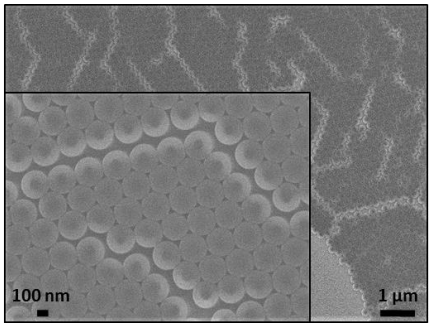

Figure 6. SEM images of nanosphere deposition results from thermal Peltier evaporation: main image at 10,000x and inset at 50,000x magnification.

3.3 Etching of Nanospheres

Exposure to oxygen plasma has shown to effectively etch polystyrene nanospheres at a controllable rate [17]. In this work, a March PX-250 Plasma Asher was used for etching. A characterization of the etch rates on the nanospheres was first performed. The resulting plot is shown in Figure 7.

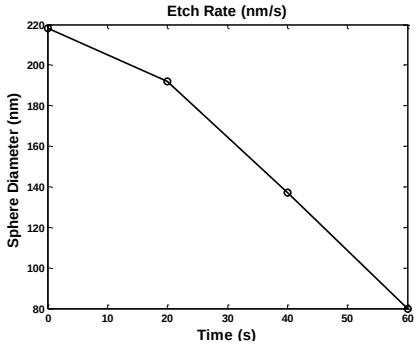

Figure 7. Oxygen plasma etch rate characterization of 200 nm polystyrene nanospheres.

Samples with deposited spheres were then etched for 43-44 seconds at a power rating of 150W, resulting in feature diameters of ~125 nm. The etched nanospheres are pictured below in Figure 8.

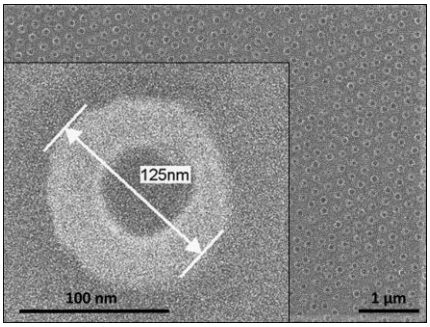

Figure 8. SEM image of nanospheres after oxygen plasma exposure.

3.4 Metal and Insulator Evaporation

Based on simulation results, a ~25 nm layer of gold, matching simulation dimensions, was deposited on the samples using a Kurt J. Lesker electron beam evaporation system, shown in Figure 9.

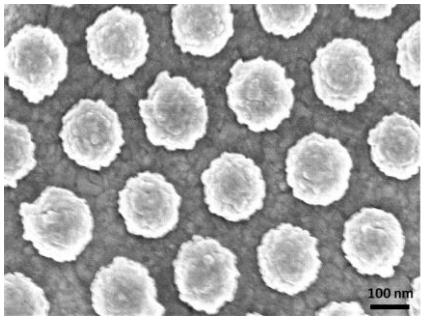

Figure 9. SEM image of nanospheres after 25 nm gold layer deposition.

Quenching effects stemming from non-radiative energy transitions in plasmonic devices is a well-known phenomenon [18]. After gold deposition, a ~8nm dielectric

spacing layer of SiO_2 was added using a Temescal BJD 2000 electron beam evaporation system to eliminate this effect.

3.5 Characterization

A solution of (CdSe/ZnS) quantum dots (QD) at a concentration of 25nM suspended in toluene was used to simulate a labeled analyte for fluorescence enhancement testing. A Ziess Violet Laser Scanning Confocal Microscope was used to view and record the emission of the QDs near the plasmonic lattice. After the QD solution was pipetted onto the device, images were acquired quickly (<5 minutes) to ensure the toluene solution did not evaporate and the QDs did not agglomerate or settle on the substrate. These images are shown in Figure 10. MATLAB scripts were used to quantify the average enhancement intensity of the device by comparing the patterned region to the unpatterned background both in the presence of the QD solution.

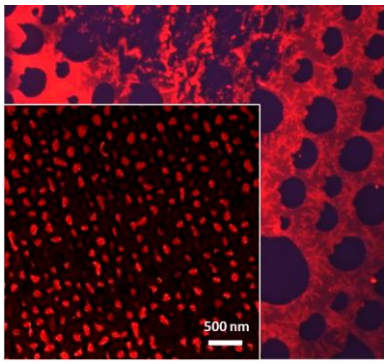

Figure 10. Optical/Confocal microscope images of fabricated PPNS in the presence of 565 nm CdSe/ZnS QD solution.

4 DISCUSSION AND CONCLUSIONS

NS fabrication has shown to offer a quick and cost-effective fabrication method in comparison to EBL, mask alignment, etc. that require multiple fabrication steps and processes to achieve similar results. A new low-cost method to fabricate plasmonic lattices for emission enhancement in biosensor architectures has been presented. Peltier evaporation was used to achieve nanosphere deposition on silicon substrates with over 85% monolayer coverage. The physical nanosphere pattern dimensions shown in this fabrication work i.e. sphere dimensions, gold layer thickness, lattice constant, etc., were based on parametric FDTD simulations. Based on simulation results, a base sphere diameter of 200 nm was easily tuned to 125 nm value using an Oxygen based plasma exposure with less than 4.5% variation in critical dimensions. A thin ~8nm spacing layer of SiO2 was added after gold layer deposition to prevent any quenching issues, from the direct interaction of the gold surface and QD solution. This approach for fabrication yielded a functional PPNS that provided a ~4-fold enhancement of CdSe/ZnS QD emission at 565 nm Further work is required to extend the etch characterization to a full array of sphere sizes, power ratings, sphere structure, exposure time, and sphere lifetime after exposure. These parameters are critical in gaining a better understanding of the nanosphere-etch relationship. Additionally, a wider range of NS sizes need to be utilized in a PPNS system to expand the known wavelength capabilities and relationships of the systems, increasing the overall merit and impact of such fabrication techniques on current and future biosensors.

Acknowledgements: M. Windam was supported by REU funding from the NSF through DMR 1559880. Additional funding was provided by the WVU Byars-Tarnay Foundation. The WVU SRF and Cleanroom were used for fabrication and characterization efforts.

5 REFERENCES

[1] Global Market Insights Inc., "Biosensors Market size set to exceed $29bn by 2024," Global Market Insights Inc. , 2016.

[2] A. Touhami, in *Nanomedicine*, One Central Press, 2014, pp. 374-403.

[3] S. P. Mohanty and E. Kougianos, *IEEE Potentials*, vol. 25, no. 2, pp. 35-40, 2006.

[4] B. R. Eggins, Chemical Sensors and Biosensors, West Sussex: John Wiley & Sons, LTD\, 2002.

[5] W. E. Moerner, *PNAS*, vol. 104, no. 31, pp. 12596-12602, 2007.

[6] W. G. Cox and V. L. Singer, *BioTechniques*, vol. 36, no. 1, pp. 114-122, 2004.

[7] R. Narayanaswamy and O. S. Wolfbeis, Optical Sensors, Berlin: Springer, 2004.

[8] M. Seydack, *Biosensors and Bioelectronics*, vol. 20, pp. 2454-2469, 2005.

[9] A. Shrivastava and V. B. Gupta, *Chronicles of Young Scientists*, vol. 2, no. 1, pp. 21-25, 2011.

[10] J. Wenger and H. Rigneault, *International Journal of Molecular Sciences*, vol. 11, pp. 206-221, 2010.

[11] M. Bauch, K. Toma, M. Toma, Q. Zhang and J. Dostalek, *Plasmonics*, vol. 9, pp. 781-799, 2014.

[12] K. Toma, E. Descrovi, M. Toma, M. Ballarini and e. all, *Biosensors and Bioelectronics*, vol. 43, pp. 108-114, 2013.

[13] S. Khatua, P. M. R. Paulo, H. Yuan, A. Gupta, P. Zijlstra and M. Orrit, *ACS Nano*, vol. 8, no. 5, pp. 4440-4449, 2014.

[14] D. Punj, R. Regmi, A. Devilez and e. all, *ACS Photonics*, vol. 2, pp. 1099-1107, 2015.

[15] K. Smith, A. Gadde, A. Kadiyala and J. M. Dawson, in *SPIE 9756*, San Francisco , 2016.

[16] M. E. Stewart, C. R. Anderton and et.all, *Chem Rev*, vol. 108, pp. 494-521, 2008.

[17] L. Li, T. Zhai, H. Zeng, X. Fang, Y. Bando and D. Golberg, *J. Mater. Chem*, vol. 21, no. 40, 2011.

[18] S. A. Maier, Plasmonics: Fundamentals and Applications, New York: Springer, 2007.